Reaction Pathway for the Direct Benzene Hydroxylation by Iron−Oxo Species

Kazunari Yoshizawa,* Yoshihito Shiota, and Tokio Yamabe

Contribution from the Department of Molecular Engineering, Kyoto University, Sakyo-ku, Kyoto 606-8501, Japan, and Institute for Fundamental Chemistry, 34-4 Takano-Nishihiraki-cho, Sakyo-ku, Kyoto 606-8103, Japan

Received May 4, 1998. Revised Manuscript Received October 23, 1998

Abstract: The direct benzene hydroxylation by an iron−oxo species is discussed from density-functional-theory (DFT) calculations. The proposed reaction pathway is $FeO^+ + C_6H_6 \rightarrow OFe^+(C_6H_6) \rightarrow$ [TS1] $\rightarrow HO-Fe^+-C_6H_5 \rightarrow$ [TS2] $\rightarrow Fe^+(C_6H_5OH) \rightarrow Fe^+ + C_6H_5OH$, in which TS means transition state. This reaction is initiated by the formation of the reactant complex, $OFe^+(C_6H_6)$, exhibiting an η^2-C_6H_6 binding mode; benzene C−H bonds are activated on this complex due to significant electron transfer from the benzene to the iron−oxo species. The reaction should proceed in a concerted manner, neither via the formation of radical species nor ionic intermediates. The reaction mechanism is quite similar to the two-step concerted mechanism that we have proposed originally for the direct methane hydroxylation by an iron−oxo species. The quartet potential energy surface affords a low-cost reaction pathway for the benzene hydroxylation, spin inversion being unimportant in contrast to the methane hydroxylation in which crossing between the sextet and quartet potential energy surfaces plays an important role. We suggest that our two-step concerted mechanism should be widely applicable to hydrocarbon hydroxylations catalyzed by transition-metal oxides if coordinatively unsaturated metal oxides are responsible for such important catalytic reactions.

Introduction

Nearly all phenol is now produced by an industrial process that starts with cumene (2-propylbenzene).[1] Cumene is converted by air oxidation into cumene hydroperoxide, which is converted by aqueous acid into phenol and acetone. Since acetone is produced as a byproduct in this process, the economics of the so-called cumene method is dependent on the marketability of acetone. Thus, economical, direct conversion of benzene to phenol has attracted the attention of researchers in pure and applied chemistry.[1b]

Such a direct benzene hydroxylation in the gas phase was investigated by Schröder and Schwarz and their collaborators.[2] The bare FeO^+ complex, which is generated from the reaction of Fe^+ with nitrous oxide (N_2O) under ion-cyclotron-resonance conditions, reacts with benzene at a collision rate of $k = 1.3 \times 10^{-9}$ cm^3/(molecule·s), giving rise to the formation of Fe^+/C_6H_5-OH (56%), $Fe(C_5H_6)^+/CO$ (37%), $Fe(C_6H_4)^+/H_2O$ (5%), and $Fe(C_5H_5)^+/CO/H^\bullet$ (2%). Detailed analyses of the gas-phase reaction clarified that MnO^+, FeO^+, and CoO^+ efficiently convert benzene to phenol whereas ScO^+, TiO^+, and VO^+ do not.[2c] It is clear from these results that the late transition-metal oxides play an essential role in the direct conversion of benzene to phenol. However, neither mechanistic nor quantum-chemical studies have yet been conducted for the very interesting gas-phase processes. An analysis of the reaction pathway is the key to understanding the catalytic benzene hydroxylation over various transition-metal oxides supported on silica gel[3] and over Fe-ZSM-5 zeolites.[4,5] Schröder and Schwarz[6] also demonstrated that the bare FeO^+ complex reacts with methane to lead to the formation of methanol in high yield. It is therefore important to investigate the reaction mechanisms for the two interesting gas-phase reactions.

Considerable theoretical work concerning C−H bond activation of small alkanes by transition-metal complexes has been conducted,[7−14] but activation of the benzene C−H bond has not yet been fully investigated from a mechanistic viewpoint. We think that the unknown reaction species that catalyzes the direct benzene hydroxylation over heterogeneous catalysts[3−5] should have relevance to transition-metal complexes including iron−oxo species by analogy with the active sites of cytochrome P450[15] and soluble methane monooxygenase (sMMO).[16] From

* To whom all correspondence should be addressed at Kyoto University. E-mail: kazunari@scl.kyoto-u.ac.jp

(1) See for example: (a) Morrison, R. T.; Boyd, R. N. *Organic Chemistry*, 6th ed.; Prentice Hall: New York, 1992; p 893. (b) *Chem. Eng. News* **1998**, *April 6*, 21.

(2) (a) Schröder, D.; Schwarz, H. *Helv. Chim. Acta* **1992**, *75*, 1281. (b) Becker, H.; Schröder, D.; Zummack, W.; Schwarz, H. *J. Am. Chem. Soc.* **1994**, *116*, 1096. (c) Ryan, M. F.; Stöckigt, D.; Schwarz, H. *J. Am. Chem. Soc*. **1994**, *116*, 9565.

(3) Iwamoto, M.; Hirata, J.; Matsukami, K.; Kagawa, S. *J. Phys. Chem*. **1983**, *87*, 665.

(4) Suzuki, E.; Nakashiro, K.; Ono, Y. *Chem. Lett.* **1988**, 953.

(5) (a) Panov, G. I.; Sheveleva, G. A.; Kharitonov, A. S.; Romannikov, V. N.; Vostrikova, L. A. *Appl. Catal. A: General* **1992**, *82*, 31. (b) Sobolev, V. I.; Kharitonov, A. S.; Paukshtis, Y. A.; Panov, G. I. *J. Mol. Catal*. **1993**, *84*, 117. (c) Sobolev, V. I.; Panov, G. I.; Kharitonov, A. S.; Romannikov, V. N.; Volodin, A. M.; Ione, K. G. *J. Catal*. **1993**, *139*, 435. (d) Panov, G. I.; Kharitonov, A. S.; Sobolev, V. I. *Appl. Catal. A: General* **1993**, *98*, 1.

(6) (a) Schröder, D.; Schwarz, H. *Angew. Chem., Int. Ed. Engl.* **1990**, *29*, 1433. (b) Schwarz, H. *Angew. Chem., Int. Ed. Engl*. **1991**, *30*, 820. (c) Schröder, D.; Fiedler, A.; Hrušák, J.; Schwarz, H. *J. Am. Chem. Soc.* **1992**, *114*, 1215. (d) Schröder, D.; Schwarz, H. *Angew. Chem., Int. Ed. Engl*. **1995**, *34*, 1973. (e) Schröder, D.; Schwarz, H.; Clemmer, D. E.; Chen, Y.-M.; Armentrout, P. B.; Baranov, V. I.; Böhme, D. K. *Int. J. Mass Spectrom. Ion Processes* **1997**, *161*, 175.

(7) (a) Saillard, J.-Y.; Hoffmann, R. *J. Am. Chem. Soc*. **1984**, *106*, 2006. (b) Hoffmann, R. *Rev. Mod. Phys*. **1988**, *60*, 601.

(8) (a) Low, J. J.; Goddard, W. A., III *J. Am. Chem. Soc*. **1984**, *106*, 8321. (b) Low, J. J.; Goddard, W. A., III *J. Am. Chem. Soc*. **1986**, *108*, 6115. (c) Perry, J. K.; Ohanessian, G.; Goddard, W. A., III *J. Phys. Chem.* **1993**, *97*, 5238.

10.1021/ja981525i CCC: $18.00
Published on Web 12/17/1998

Scheme 1

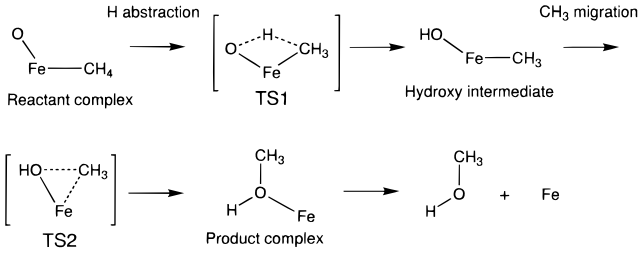

previous work,[17] we believe that the direct benzene hydroxylation catalyzed by the FeO^+ complex should occur following the two-step concerted mechanism (Scheme 1) that we have proposed originally for the methane hydroxylation. Our recent interest is in whether the concerted mechanism is applicable to hydrocarbon hydroxylations catalyzed by the metalloenzymes in which the coordination environment would dominate the mechanism and selectivity. We have proposed from theoretical calculations[18] that the conversion of methane to methanol can occur on a diiron site of sMMO similar to the gas-phase reaction indicated in Scheme 1.

In this work, we present from density-functional-theory (DFT) calculations how the iron−oxo species activates benzene to lead to the formation of phenol. The reaction intermediates and the energetics along the reaction pathway are computed and analyzed in detail. Orbital interaction analyses are performed to gain a better understanding of the important reaction, especially concerning the reason a certain spin state plays an essential role. Our theoretical analysis on the direct benzene hydroxylation will probably be influential among experimentalists in the fields of catalysis chemistry as well as of bioinorganic chemistry.

Method of Calculation

We optimized local minima (on a potential energy surface) corresponding to the reactant complex, $OFe^+(C_6H_6)$, the reaction intermediate, $HO-Fe^+-C_6H_5$, and the product complex, $Fe^+(C_6H_5OH)$, using the hybrid Hartree−Fock/density-functional-theory (HF/DFT) B3LYP method.[19,20] This method consists of the Slater exchange, the Hartree−Fock exchange, the exchange functional of Becke,[19] the correlation functional of Lee, Yang, and Parr (LYP),[20] and the correlation functional of Vosco, Wilk, and Nusair.[21] The contribution of each energy to the B3LYP energy expression was fitted by Becke[19] empirically on a reference set of molecules. The hybrid B3LYP method has been reported to provide excellent descriptions of various reaction profiles, particularly in geometries, heats of reaction, barrier heights, and vibrational analyses.[22]

For the Fe atom we used the (14s9p5d) primitive set of Watchers[23] supplemented with one polarization f-function ($\alpha = 1.05$)[24] resulting in a (611111111|51111|311|1) [9s5p3d1f] contraction, and for the H, C, N, and O atoms we used the D95** basis set,[25] a standard double-ζ basis set with polarization function. Transition-state (TS) structures were also optimized at the same level of theory. Vibrational frequencies were systematically computed to ensure that on a potential energy surface each optimized geometry corresponds to a local minimum that has no imaginary frequency or a saddle point that has only one imaginary frequency. Zero-point energy corrections were taken into account in calculating the total energies of the reactant complex, the intermediate, the product complex, and the transition states. Sextet and quartet spin states were considered. The spin-unrestricted method was applied to the open-shell systems. Computed $\langle S^2 \rangle$ values confirmed that spin contamination included in calculations was very small (within 0.3% after annihilation of spin contamination). The Gaussian 94 program package was used for all DFT calculations.[26]

One of the reviewers of this paper suggested we include some calibration calculations to evaluate the applicability of the method we used. We list in Table 1 computed values for the dissociation energy of the $^6\Sigma^+$ state of FeO^+ at various levels of theory as well as an experimental value. The B3LYP method behaves quite well for this quantity to give a value comparable to the experimental value. Thus, this hybrid DFT method is appropriate for the subject of this paper, the reaction between FeO^+ and benzene.

We performed orbital interaction analyses, based on the extended Hückel method[29] to have a deeper understanding of the reaction profile

(9) (a) Blomberg, M. R. A.; Brandemark, U.; Siegbahn, P. E. M. *J. Am. Chem. Soc*. **1983**, *105*, 5557. (b) Blomberg, M. R. A.; Siegbahn, P. E. M.; Nagashima, U.; Wennerberg, J. *J. Am. Chem. Soc*. **1991**, *113*, 424. (c) Blomberg, M. R. A.; Siegbahn, P. E. M.; Svensson, M. *J. Am. Chem. Soc*. **1992**, *114*, 6095. (d) Siegbahn, P. E. M.; Blomberg, M. R. A. *Organometallics* **1994**, *13*, 354. (e) Siegbahn, P. E. M. *Organometallics* **1994**, *13*, 2833. (f) Siegbahn, P. E. M. *J. Am. Chem. Soc.* **1996**, *118*, 1487. (g) Siegbahn, P. E. M.; Crabtree, R. H. *J. Am. Chem. Soc.* **1996**, *118*, 4442.

(10) (a) Ziegler, T.; Tschinke, V.; Becke, A. D. *J. Am. Chem. Soc*. **1987**, *109*, 1351. (b) Ziegler, T.; Tschinke, V.; Fan, L.; Becke, A. D. *J. Am. Chem. Soc*. **1989**, *111*, 9177. (c) Ziegler, T.; Folga, E.; Berces, A. *J. Am. Chem. Soc*. **1993**, *115*, 636.

(11) (a) Koga, N.; Morokuma, K. *J. Phys. Chem.* **1990**, *94*, 5454. (b) Koga, N.; Morokuma, K. *J. Am. Chem. Soc*. **1993**, *115*, 6883. (c) Musaev, D. G.; Koga, N.; Morokuma, K. *J. Phys. Chem*. **1993**, *97*, 4064. (d) Musaev, D. G.; Morokuma, K.; Koga, N.; Ngyen, K.; Gordon, M. S.; Cundari, T. R. *J. Phys. Chem*. **1993**, *97*, 11435. (e) Musaev, D. G.; Morokuma, K. *J. Chem. Phys*. **1994**, *101*, 10697. (f) Musaev, D. G.; Morokuma, K. *J. Phys. Chem*. **1996**, *100*, 11600.

(12) (a) Sakaki, S.; Ieki, M. *J. Am. Chem. Soc.* **1991**, *113*, 5063. (b) Sakaki, S.; Ieki, M. *J. Am. Chem. Soc.* **1993**, *115*, 2373.

(13) (a) Cundari, T. R. *J. Am. Chem. Soc.* **1992**, *114*, 10557. (b) Cundari, T. R.; Gordon, M. S. *J. Am. Chem. Soc.* **1993**, *115*, 4210. (c) Cundari, T. R. *J. Am. Chem. Soc*. **1994**, *116*, 340.

(14) (a) Holthausen, M. C.; Koch, W. *Helv. Chim Acta* **1996**, *79*, 1939. (b) Holthausen, M. C.; Koch, W. *J. Am. Chem. Soc*. **1996**, *118*, 9932. (c) Holthausen, M. C.; Hornung, G.; Schröder, D.; Sen, S.; Koch, W.; Schwarz, H. *Organometallics* **1997**, *16*, 3135. (d) Sändig, N.; Koch, W. *Organometallics* **1997**, *16*, 5242.

(15) (a) *Cytochrome P450: Structure, Mechanism, and Biochemistry*, 2nd ed.; Ortiz de Montellano, P. R., Ed.; Plenum: New York, 1995. (b) Sono, M.; Roach, M. P.; Coulter, E. D.; Dawson, J. H. *Chem. Rev.* **1996**, *96*, 2841.

(16) (a) Kurtz, D. M., Jr. *J. Biol. Inorg. Chem.* **1997**, *2*, 159. (b) Wallar, B. J.; Lipscomb, J. D. *Chem. Rev.* **1996**, *96*, 2625. (c) Que, L., Jr.; Dong, Y. *Acc. Chem. Res.* **1996**, *29*, 190. (d) Feig, A. L.; Lippard, S. J. *Chem. Rev.* **1994**, *94*, 759. (e) Lipscomb, J. D. *Annu. Rev. Microbiol*. **1994**, *48*, 371. (f) Lippard, S. J. *Angew. Chem., Int. Ed. Engl.*, **1988**, *27*, 344.

(17) (a) Yoshizawa, K.; Shiota, Y.; Yamabe, T. *Chem. Eur. J.* **1997**, *3*, 1160. (b) Yoshizawa, K.; Shiota, Y.; Yamabe, T. *J. Am. Chem. Soc.* **1998**, *120*, 564.

(18) (a) Yoshizawa, K. *J. Biol. Inorg. Chem.* **1998**, *3*, 318. (b) Yoshizawa, K.; Hoffmann, R. *Inorg. Chem*. **1996**, *35*, 2409. (c) Yoshizawa, K.; Yamabe, T.; Hoffmann, R. *New J. Chem.* **1997**, *21*, 151. (d) Yoshizawa, K.; Yokomichi, Y.; Shiota, Y.; Ohta, T.; Yamabe, T. *Chem. Lett.* **1997**, 587. (e) Yoshizawa, K.; Ohta, T.; Shiota, Y.; Yamabe, T. *Chem. Lett.* **1997**, 1213. (f) Yoshizawa, K.; Ohta, T.; Yamabe, T.; Hoffmann, R. *J. Am. Chem. Soc.* **1997**, *119*, 12311. (g) Yoshizawa, K.; Ohta, T.; Yamabe, T. *Bull. Chem. Soc. Jpn.* **1998**, *71*, 1899.

(19) (a) Becke, A. D. *Phys. Rev.* **1988**, *A38*, 3098. (b) Becke, A. D. *J. Chem. Phys*. **1993**, *98*, 5648.

(20) Lee, C.; Yang, W.; Parr, R. G. *Phys. Rev.* **1988**, *B37*, 785.

(21) Vosco, S. H.; Wilk, L.; Nusair, M. *Can. J. Phys*. **1980**, *58*, 1200.

(22) Baker, J.; Muir, M.; Andzelm, J.; Scheiner A. In *Chemical Applications of Density-Functional Theory*; Laird, B. B., Ross, R. B., Ziegler, T., Eds.; ACS Symp. Ser. 629; American Chemical Society: Washington, DC, 1996.

(23) Wachters, A. J. H. *J. Chem. Phys*. **1970**, *52*, 1033.

(24) Raghavachari, K.; Trucks, G. W. *J. Chem. Phys*. **1989**, *91*, 1062.

(25) Dunning, T. H.; Hay, P. J. In *Modern Theoretical Chemistry*; Schaefer, H. F., Ed.; Plenum: New York, 1976.

(26) Frisch, M. J.; Trucks, G. W.; Schlegel, H. B.; Gill, P. M. W.; Johnson, B. G.; Robb, M. A.; Cheeseman, J. R.; Keith, T. A.; Petersson, G. A.; Montgomery, J. A.; Raghavachari, K.; Al-Laham, M. A.; Zakrzewski, V. G.; Ortiz, J. V.; Foresman, J. B.; Cioslowski, J.; Stefanov, B. B.; Nanayakkara, A.; Challacombe, M.; Peng, C. Y.; Ayala, P. Y.; Chen, W.; Wong, M. W.; Andres, J. L.; Replogle, E. S.; Gomperts, R.; Martin, R. L.; Fox, D. J.; Binkley, J. S.; Defrees, D. J.; Baker, J.; Stewart, J. J. P.; Head-Gordon, M.; Gonzalez, C.; Pople, J. A. *Gaussian 94*; Gaussian Inc.: Pittsburgh, PA, 1995.

(27) Fiedler, A.; Hrušák, J.; Koch, W.; Schwarz, H. *Chem. Phys. Lett.* **1993**, *211*, 242.

Table 1. Dissociation Energies (in kcal/mol) of the $^6\Sigma^+$ State of FeO^+ from Computations at Various Levels of Theory and from Experiment

method	dissociation energy
MP2(FC)	40.8[a]
MP4(FC)	44.2[a]
CISD+D(FC)	33.6[a]
CCSD(T)(FC)	64.7[a]
QCISD(T)(FC)	72.2[a]
CASSCF	25.4[a]
MRCI+D(FC)	70.2[a]
CASPT2N(full)	74.6[a]
B3LYP	75.2[b]
exptl	81.4 ± 1.4[c]

[a] Cited from ref 27. [b] This study. [c] Cited from ref 28.

of the direct conversion of benzene to phenol, particularly with regard to the barrier heights of transition states with different spin states. We used the YAeHMOP program developed by Landrum.[30]

Results and Discussion

Reaction Intermediates and Transition States. Let us consider the gas-phase reaction of FeO^+ and benzene. As mentioned above, this reaction leads to the formation of phenol in a high yield of 56%.[2] This reaction can be viewed as a simple model for the catalytic benzene hydroxylation over Fe-ZSM-5 zeolites if we assume that the unknown reaction species has relevance to the iron−oxo species. We confirmed from DFT calculations that the conversion of benzene to phenol by FeO^+ is initiated by C−H activation of benzene which occurs through the formation of the reactant complex, $OFe^+(C_6H_6)$. A subsequent H atom abstraction from the benzene, via four-centered TS1, results in formation of the hydroxy intermediate, $HO-Fe^+-C_6H_5$. This important intermediate is finally transformed into the product complex, $Fe^+(C_6H_5OH)$, via three-centered TS2, followed by dissociation into phenol and Fe^+. The proposed reaction pathway, indicated in reaction 1, is quite similar to that of the methane−methanol conversion by MnO^+, FeO^+, and CoO^+.[17] It is important to note that in the initial stages of the proposed reaction pathway we rule out a direct H atom abstraction by the oxygen atom of the iron−oxo species. Our mechanism is different from a conventional radical mechanism that involves a direct H atom abstraction with a linear C−H−OFe array.

$$FeO^+ + C_6H_6 \rightarrow OFe^+(C_6H_6) \rightarrow [TS1] \rightarrow HO-Fe^+-C_6H_5 \rightarrow [TS2] \rightarrow Fe^+(C_6H_5OH) \rightarrow Fe^+ + C_6H_5OH \quad (1)$$

The three reaction intermediates and the two transition states along the reaction pathway on the sextet potential energy surface are shown in Figure 1. Systematic vibrational analyses confirmed that the reactant complex, the hydroxy intermediate, and the product complex correspond to stable points on the potential energy surface and that TS1 and TS2 correspond to saddle points. The geometries of the reaction intermediates and the transition states are quite similar in the sextet- and quartet-spin states.

Let us first look at the computed geometry of the reactant complex, $OFe^+(C_6H_6)$, in detail. There are in general three typical binding modes for a metal−benzene complex: the η^6-, η^4-, and η^2-C_6H_6 modes, as indicated in **1**, **2**, and **3**, respectively. Interconversion of these is expected to occur.[31] We found from a vibrational analysis that an optimized $OFe^+(\eta^6\text{-}C_6H_6)$ complex exhibits a 2-fold degenerate imaginary-frequency mode; thus this structure is not a stable point on the potential energy surface. We predict from DFT computations that the Fe atom is closer to one pair of carbon atoms, as indicated in Figure 1; the two Fe−C distances of 2.324 and 2.344 Å are clearly shorter than other Fe−C distances lying within a range of 2.467−2.658 Å. Thus, this initially formed species can be viewed as an $OFe^+(\eta^2\text{-}C_6H_6)$ complex, in which the benzene ring remains nearly planar. The computational results are consistent with the general features of the M−benzene complexes with an η^2-coordination mode reported in previous papers,[32] in which M is bare transition metals and their ions such as Pt and Ag^+. Thus, the structure of the reactant complex should follow the generally accepted picture of the bonding in π complexes in terms of electron donation from filled bonding π orbitals of the benzene and simultaneous electron acceptance into empty antibonding π^* orbitals; such bonding interactions may be generally drawn from the Dewar−Chatt−Duncanson bonding model.[33] Computed binding energies of 59.9 kcal/mol in the sextet state and 67.7 kcal/mol in the quartet state of the $OFe^+(C_6H_6)$ complex are much larger than those (22.8 and 22.2 kcal/mol) of the $OFe^+(CH_4)$ complex.[17b]

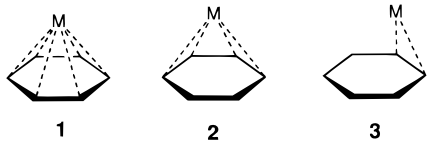

Figure 2 shows orbital interaction analyses for the $OFe^+(\eta^6\text{-}C_6H_6)$ and $OFe^+(\eta^2\text{-}C_6H_6)$ complexes, in which we assume the benzene ring to be a D_{6h} structure to derive simpler orbital interactions. The FMO (fragment molecular orbital) diagrams are built up from the FeO^+ species (in its high-spin d^5 configuration) and the benzene. The high-lying 1δ, 2π, and 3σ orbitals of the FeO^+ fragment consist mainly of 3d atomic orbitals of the iron, and the low-lying 2σ and 1π orbitals (not shown here) come mainly from 2p atomic orbitals of the oxygen. At the center in Figure 2 the five d-block orbitals of the FeO^+ fragment are shown; on the left the orbitals reconstructed for the $OFe^+(\eta^6\text{-}C_6H_6)$ complex are demonstrated; on the right the orbitals for the $OFe^+(\eta^2\text{-}C_6H_6)$ complex are shown. The orbitals for the two binding modes are demonstrated in their high-spin d^5 configuration.

In the η^6-C_6H_6 mode the degenerate 2π of the FeO^+ fragment has good interaction with the 2-fold degenerate HOMO of the benzene fragment so that the in-phase combination is stabilized to −13.2 eV and the out-of-phase counterpart is pushed up to −11.2 eV. Other orbitals of the two fragments do not mix with each other in this binding mode, due to orbital symmetry. Therefore both the sextet and quartet states in the η^6-C_6H_6 mode are energetically unfavorable because the destabilized orbitals are doubly and singly occupied in the sextet and quartet states,

(28) Loh, S. K.; Fisher, E. R.; Lian, L.; Schultz, R. H.; Armentrout, P. B. *J. Phys. Chem.* **1989**, *93*, 2601.
(29) (a) Hoffmann, R. *J. Chem. Phys*. **1963**, *39*, 1397. (b) Hoffmann, R.; Lipscomb, W. N. *J. Chem. Phys.* **1962**, *36*, 2179; **1962**, *37*, 2872.
(30) Landrum. G. A. *YAeHMOP* (*Yet Another Extended Hückel Molecular Orbital Package*), Version 2.0; Cornell University: Ithaca, New York, 1997.
(31) Muetterties, E. L.; Bleeke, J. R.; Wucherer, E. J.; Albright, T. A. *Chem. Rev*. **1982**, *82*, 499.
(32) (a) Bauschlicher, C. W.; Partridge, H.; Langhoff, S. R. *J. Phys. Chem.* **1992**, *96*, 3273. (b) Roszak, S.; Balasubramanian, K. *Chem. Phys. Lett.* **1995**, *234*, 101.
(33) (a) Dewar, M. J. S. *Bull. Soc. Chim. Fr*. **1951**, *18*, C71. (b) Chatt, J.; Duncanson, L. A. *J. Chem. Soc.* **1953**, 2939.

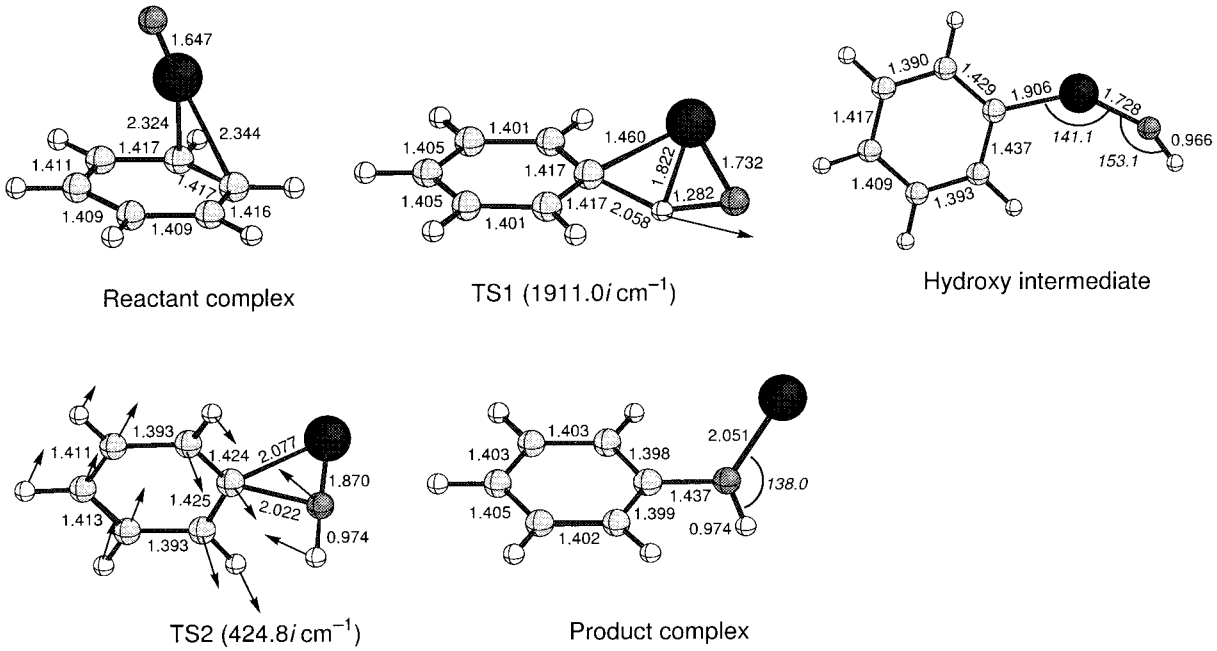

Figure 1. Reaction intermediates and transition states for the direct benzene hydroxylation by the FeO^+ species in the sextet state. Bond lengths are in Å and bond angles (italic) are in deg.

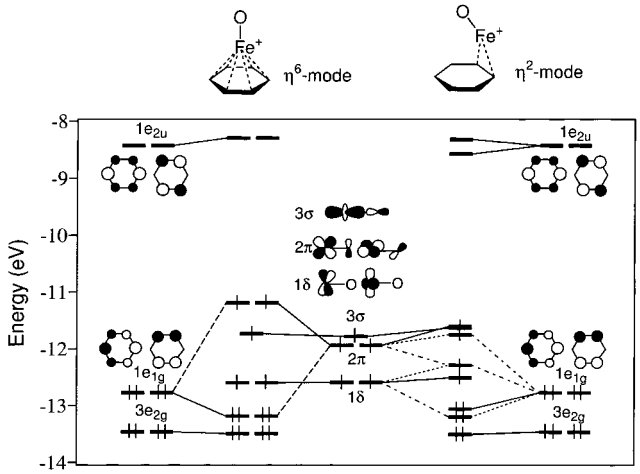

Figure 2. Orbital interaction analyses for the initially formed OFe^+-(η^6-C_6H_6) and OFe^+(η^2-C_6H_6) complexes on the left and right, respectively. The geometry of the benzene is idealized to be D_{6h} symmetry, in which the HOMO and LUMO are 2-fold degenerate.

respectively. In contrast, the orbital interactions in the η^2-C_6H_6 mode are a little complicated, but we understand from a close inspection of the FMO diagrams that the η^2-C_6H_6 mode is preferred to the η^6-C_6H_6 mode because the 2π of the FeO^+ fragment is not significantly destabilized in the η^2-C_6H_6 mode. In this way, our qualitative orbital interaction analyses reasonably explain the DFT result that the η^2-C_6H_6 mode is energetically preferred.

The degenerate LUMO of the benzene fragment remains almost unchanged in energy because it does not mix with the d-block orbitals of the FeO^+ fragment. The dominant interaction in this π complex is therefore in electron donation from the filled bonding π orbital of the benzene, and the degree of back-donation is small, as demonstrated in Figure 2. The total charge of the benzene ring is thus +0.23 from DFT computations. Consequently, the C−C bonds of the benzene ring are slightly longer than that of 1.403 Å in free benzene as shown in Figure 1, but the C−H bond lengths are not different from that of 1.089 Å in free benzene. We think that benzene activation occurs initially through the formation of this π reactant complex. Before conducting computations, we expected a σ-type complex, in which FeO^+ is strongly bound to a single carbon atom and as a result the benzene ring is deformed from a plane, but we could not find such a σ-complex as a stable structure on the potential energy surface.

TS1, which connects the reactant complex and the hydroxy intermediate, exhibits an imaginary frequency of 1911*i* cm^{-1}, the vibrational mode of which is indicated by the arrow in Figure 1. This high frequency is a direct consequence of C−H bond cleavage as well as a O−H bond formation, as the vibrational mode suggests. The C−H bond and the O−H bond in the four-centered structure were computed to be 1.460 and 1.282 Å, respectively. These values are reasonable for a transition-state structure responsible for a C−H bond breaking and an O−H bond forming. The C−H bond is significantly deviated from the benzene plane; the four-centered structure is orthogonal to the benzene plane. The structure of TS1 reminds us of the famous σ complex or arenium ion,[34] a highly reactive intermediate in aromatic electrophilic substitution. Although in theoretical chemistry a reaction intermediate is strictly defined as a local minimum on a potential energy surface, its definition is sometimes not so precise in experimental chemistry.

We next take a look at the hydroxy intermediate, HO−Fe^+−C_6H_5 in Figure 1. This intermediate is likely to play a central role in the reaction pathway for the benzene−phenol conversion, by analogy with the reaction pathway for the methane−methanol conversion. The FeOH moiety is nearly coplanar with the benzene ring. The formation of the Fe−C bond significantly affects the two C−C bonds adjacent to it and consequently these C−C bond lengths, which were computed to be 1.437 and 1.429 Å, are much larger than others. Clearly, the Fe−O bond of 1.728 Å is shorter than the expected distance of about 2 Å for a coordinate Fe−O bond. Since the Mulliken charge of the OH moiety is −0.39, this short Fe−O distance seems to be reasonable; we mean that this bond should be viewed as a covalent bond, not a coordinate bond. The formation of this

(34) See for example: March, J. *Advanced Organic Chemistry*, 4th ed.; John Wiley & Sons: New York, 1992; p 501.

intermediate may have relevance to the mechanism of *Gif* chemistry proposed by Barton and collaborators,[35] but to the best of our knowledge *Gif* chemistry does not mention how such an interesting Fe−C bond is formed in the initial stages of the proposed mechanism.

TS2 is a transition state in which Fe−C bond breaking and C−O bond formation occur simultaneously to connect the hydroxy intermediate and the product complex, $Fe^+(C_6H_5OH)$, including phenol as a ligand. This three-centered transition state can be viewed as a process for a phenyl migration from the iron active center to the oxygen atom. It exhibits an imaginary frequency of 425*i* cm^{-1}, which is lower than that of TS1, because TS2 is concerned with a coupling of the OH and C_6H_5 fragments in contrast to TS1 which is responsible for C−H bond cleavage as well as O−H bond formation. The breaking Fe−C bond and the forming C−O bond were computed reasonably well to be 2.077 and 2.022 Å, respectively. The three-centered (Fe,O,C) structure responsible for the phenyl migration is orthogonal with the benzene ring as in TS1.

Let us finally look at the product complex, $Fe^+(C_6H_5OH)$. Note that the basic structure of the phenol moiety in the product complex is not significantly changed from that of isolated phenol. The Fe−O distance of 2.051 Å is much longer than those of the reactant complex and the hydroxy intermediate. The Fe−O bond of the product complex is thus viewed as a typical coordinate bond in contrast to those of the reactant complex and the hydroxy intermediate, as indicated in Figure 1. Thus, we expect that the Fe−O bond in the product complex should easily dissociate to lead to the final products, i.e., phenol and Fe^+. The contrast between the Fe−O bonds in the hydroxy intermediate and the product complex is interesting.

Since the geometries of the intermediate species and the transition states in the low-spin quartet state are basically identical with those in the high-spin sextet state, we will not discuss them further. The only variation in their geometries is the bond distances around the Fe atom; the Fe−C and Fe−O distances in the reactant complex, the hydroxy intermediate, and the product complex in the low-spin quartet state are 0.04−0.2 Å shorter than those in the sextet state. These computational results are reasonably consistent with the general features of metal−ligand distances in high-spin and low-spin complexes.

Energetics of the Reaction Pathway. The computed sextet and quartet potential energy diagrams along the pathway of reaction 1 are shown in Figure 3. From an inspection of the two diagrams, we expect that the quartet potential surface should afford an energetically low-cost reaction pathway whereas the sextet state is important in the entrance and exit channels. Although crossing between the two potential energy surfaces occurs twice in the vicinity of the reactant and product complexes, the spin inversions have little effect on the energetics of the reaction pathway because the sextet and quartet energies at the three stable points, i.e., the reactant complex, the hydroxy intermediate, and the product complex, are close in energy. Only the barrier heights for the transition states of different spin states are crucial for the characterization of the direct benzene hydroxylation. Therefore only the quartet potential surface is likely to play an essential role in this reaction because the barrier heights of TS1 and TS2 on the quartet potential surface are smaller. This situation is somewhat different from that of the reaction pathway for the methane-to-methanol conversion by FeO^+,[17] in which such spin inversions in the entrance and exit channels play a significant role.

(35) (a) Barton, D. H. R.; Doller, D. *Acc. Chem. Res.* **1992**, *25*, 504. (b) Barton, D. H. R.; Hu, B. *Pure Appl. Chem.* **1997**, *69*, 1941.

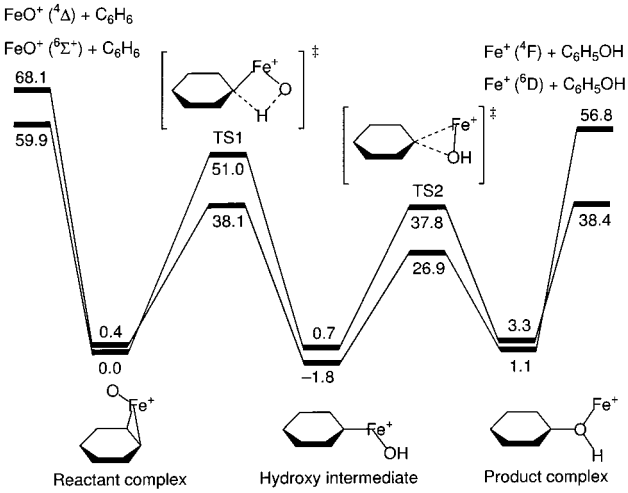

Figure 3. Potential energy diagrams for the direct benzene hydroxylation by the FeO^+ species in the sextet and quartet states. Note that the reaction proceeds in a two-step manner, via TS1 and TS2. Relative values are in kcal/mol.

On the quartet potential surface, the activation barrier for the C−H bond cleavage via TS1 was computed to be 37.7 kcal/mol, and that for the Fe−C bond cleavage via TS2 28.7 kcal/mol. The crossing between the sextet and quartet surfaces does not play a role in the benzene hydroxylation, as mentioned above. It is interesting to compare the activation energies as well as the reaction mechanism with those in the methane−methanol conversion by FeO^+.[24] In the methane hydroxylation, the corresponding barrier height for TS1 was computed to be 31.1 and 15.7 kcal/mol on the sextet and quartet potential energy surface, respectively, and it becomes 22.1 kcal/mol if we consider a crossing between the sextet and quartet surfaces.[17b] Thus, the spin inversion plays an important role in decreasing the activation energy for the C−H bond cleavage of methane. The barrier height for TS2 in the methane hydroxylation is 36.2 and 28.6 kcal/mol in the sextet and quartet states, respectively. In any event, the general features of the reaction pathways as well as the energetics of the two important reactions, the methane and benzene hydroxylations, are quite similar.

Orbital Interactions in the C−H Activation of Benzene. We conducted an FMO analysis for TS1 to consider the reason the low-spin quartet state affords a flat potential energy surface compared with the sextet state. Application of such an orbital interaction analysis to the transition state is very effective for the characterization of transition states with different spin states, as we will show below. The structure of TS1, shown in Figure 1, can be theoretically partitioned into FeO^+ and benzene fragments. Figure 4 illustrates an FMO analysis of TS1, in which the d-block levels of the FeO^+ species are shown on the left, the frontier orbitals of the deformed benzene on the right, and the orbitals reconstructed from the two fragments at the center. The HOMO of the benzene fragment interacts well with a few of the d-block orbitals of the FeO^+ fragment.

As a consequence, the 3σ orbital of the FeO^+ fragment in TS1 is significantly pushed up to −10.7 eV; in the sextet state this orbital is singly occupied, but in the quartet state it is empty. Although explicit electron−electron interactions are not included in the extended Hückel method,[29] we can have some information about a preferred spin state from an empirical criterion within the framework of this one-electron theory; a low-spin state is expected in general to occur in the extended Hückel method if an energy splitting between two levels is more than 1.5 eV.[36] This d-block orbital at −10.7 eV lies just 1.5 eV above the

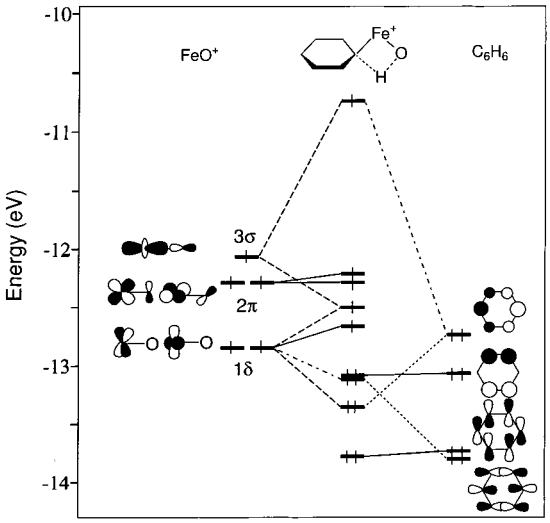

Figure 4. An orbital interaction analysis for the concerted H atom abstraction of benzene (TS1). The electronic configurations indicated at the left and center are high-spin sextet states.

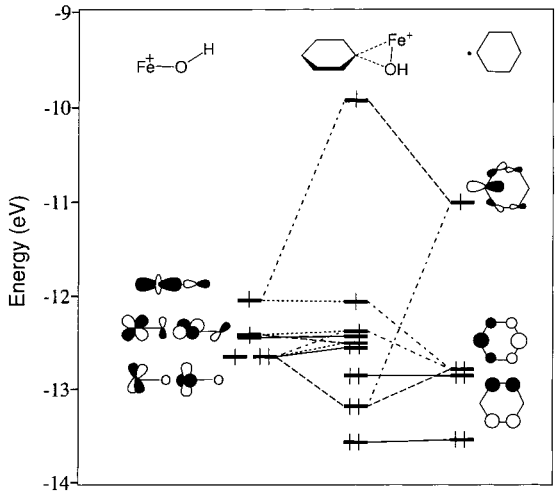

Figure 5. An orbital interaction analysis for the concerted phenyl migration (TS2). The electronic configuration indicated at the center is a sextet spin state.

next high-lying orbital, as shown in Figure 4, so that the sextet state of TS1 is comparable to the corresponding quartet state in energy within the framework of the one-electron theory.

Another important result can be derived from the FMO analysis in Figure 4. We expect that d^4-oxo complexes, e.g., MnO^+ and FeO^{2+}, should be more efficient for the activation of the C−H bond of benzene because in the quintet state of TS1 the high-lying d-block orbital at −10.7 eV is unfilled and the other low-lying d-block orbitals are singly occupied by four electrons. In addition, exchange interactions among the four electrons with the same spin can work well to stabilize the high-spin quintet state of TS1 so that we can derive this statement. In previous papers,[17b,37] we demonstrated from DFT calculations that this qualitative prediction is true in the methane-to-methanol conversion by the bare transition-metal oxides; the activation barriers of TS1 in the MnO^+ and FeO^{2+} cases were calculated to be only 9.4 and 4.9 kcal/mol, respectively, while that in the FeO^+ case is 22.1 kcal/mol. Thus, we expect that bare d^4-oxo complexes activate the C−H bond of hydrocarbons most efficiently, but it is important to note that all the hydroxylations are dependent on the barrier heights of both TS1 and TS2. Although iron(IV)−oxo complexes play an essential role in hydroxylase enzymes such as cytochrome P450[14] and sMMO,[15] such iron(IV) species have not yet been detected in Fe-ZSM-5 zeolites. Of course, our qualitative discussion based on orbital interaction analyses depends on the coordination spheres of the metal active center. However, if coordinatively unsaturated iron is generated in catalytic or enzymatic systems to afford a coordination site for substrate hydrocarbons, we expect that similar reactions should occur along the reaction pathway presented in Figure 3.[18a,g]

Let us next consider the orbital interactions in TS2. It is wise to partition TS2 into the $FeOH^+$ and $C_6H_5^\bullet$ fragments. We show an FMO analysis in Figure 5. The five d-block orbitals of the $FeOH^+$ fragment, which are similar to those of FeO^+, are occupied by six electrons, and the radical orbital of the $C_6H_5^\bullet$ fragment at −11 eV, which directs toward the missing H atom, is singly occupied. The orbital degeneracy of the $FeOH^+$ fragment shown on the left in Figure 5 is accidental. We can reconstruct the molecular orbitals of TS2 from these fragment molecular orbitals, as shown at the center of the illustration. The sextet and quartet states can be reasonably composed of ferromagnetic and antiferromagnetic couplings of the quintet state of the $FeOH^+$ fragment and the doublet state of the $C_6H_5^\bullet$ fragment, respectively. The high-lying orbital at −10 eV, which comes mainly from the $C_6H_5^\bullet$ radical orbital at −11 eV, is occupied by one electron in the sextet state of TS2, as shown at the center in Figure 5. On the other hand, the high-lying orbital is empty in the quartet state. The energy separation between the high-lying d-block orbital and the low-lying d-block orbitals is more than 2 eV and therefore the quartet state of TS2 is predicted to be energetically more stable than the corresponding sextet state from the criterion of the extended Hückel method mentioned above. From the one-electron picture, we can thus qualitatively understand why the quartet state of TS2 is energetically more stable than the sextet state. In this way, FMO analyses are quite useful for a qualitative understanding of the reaction profile, especially for transition states TS1 and TS2.

Conclusions

We propose a concerted reaction pathway for the direct benzene hydroxylation by an iron−oxo species. The reaction occurs through concerted H atom and phenyl migrations at the iron active center, neither via the formation of radical species nor ionic intermediates. The conversion of benzene to phenol by the FeO^+ species is initiated by C−H activation of benzene, which occurs through the formation of the reactant complex, $OFe^+(C_6H_6)$. Detailed DFT computations and orbital interaction analyses predict that the reactant π complex should prefer an η^2-C_6H_6 mode rather than an η^6-C_6H_6 mode; the formation of Fe−C bonds in the $OFe^+(\eta^2$-$C_6H_6)$ complex plays an essential role in the C−H bond activation in the initial stages of the reaction. A subsequent H atom abstraction from the benzene ring in the π complex, which occurs via four-centered TS1, results in the formation of the hydroxy intermediate, HO−Fe^+−C_6H_5. This stable intermediate is in the next step transformed into the product complex, $Fe^+(C_6H_5OH)$, via three-centered TS2 responsible for a phenyl migration, followed by dissociation into phenol and Fe^+. Some important energies along the reaction

(36) Hoffmann, R.; Zeiss, G. D.; Van Dine, G. W. *J. Am. Chem. Soc.* **1968**, *90*, 1485.

(37) Yoshizawa, K.; Shiota, Y.; Yamabe, T. *Organometallics* **1998**, *17*, 2825. In this paper, a concerted H atom abstraction via TS1 in Scheme 1 was shown to be energetically more favorable than a direct H atom abstraction via a transition state with a linear C−H−OFe array.

Table 2. Computed Binding Energies, Activation Energies for TS1 (ΔE_1) and TS2 (ΔE_2), and Desorption Energies (in kcal/mol) for the Conversion of Benzene to Phenol along Eq 1

spin state	binding energy	ΔE_1	ΔE_2	desorption energy
sextet	59.9	51.0	37.1	35.1
quartet	67.7	37.7	28.7	57.9

pathway are listed in Table 2. The proposed reaction mechanism is essentially identical with that of the methane−methanol conversion by coordinatively unsaturated iron−oxo species. Our two-step concerted mechanism should be widely applied to hydrocarbon hydroxylations catalyzed by transition-metal oxides if metal oxides are responsible for such important catalytic reactions. The reaction pathway for the direct benzene hydroxylation discussed in this paper may increase our understanding of some catalytic and enzymatic processes concerning aromatic-ring oxidations by various transition-metal oxides.

Acknowledgment. We are grateful to a Grant-in-Aid for Scientific Research on Priority Area "Molecular Biometallics" from the Ministry of Education, Science, Sports and Culture, Japan and to "Research for the Future" Program from the Japan Society for the Promotion of Science (JSPS-RFTF96P00206) for their support of this work. Computations were partly carried out at the Supercomputer Laboratory of Kyoto University and at the Computer Center of the Institute for Molecular Science.

Appendix

Extended Hückel parameters for Fe, O, C, and H atoms are given in Table 3.

Table 3. Extended Hückel Parameters for Fe, O, C, and H Atoms, in Which H_{ii} Is the Orbital Energy and ζ the Slater Exponent

orbital	H_{ii} (eV)	ζ_1	c_1	ζ_2	c_2
Fe4s	−9.1	1.9			
Fe4p	−5.32	1.9			
Fe3d	−12.6	5.35	0.5505	2.00	0.6260
O2s	−32.3	2.275			
O2p	−14.8	2.275			
C2s	−21.4	1.625			
C2p	−11.4	1.625			
H1s	−13.6	1.3			

JA981525I